Accepted Manuscript

Chemical Science

Dynamic Article Links▶

EDGE ARTICLE

Electrocatalytic CO$_2$ Reduction by M(bpy-R)(CO)$_4$ (M = Mo, W; R = H, *t*Bu) Complexes. Electrochemical, Spectroscopic, and Computational Studies and Comparison with Group 7 Catalysts.

Melissa L. Clark,[a] **Kyle A. Grice,**[‡a] **Curtis E. Moore, Arnold L. Rheingold, and Clifford P. Kubiak***

The tetracarbonyl molybdenum and tungsten complexes of 2,2'-bipyridine and 4,4'-di-*tert*-butyl-2,2'-bipyridine (M(bpy-R)(CO)$_4$; R = H, M = Mo (**1**), W (**2**); R = *t*Bu, M = Mo (**3**), W (**4**)) are found to be active electrocatalysts for the reduction of CO$_2$. The crystal structures of M(bpy-*t*Bu)(CO)$_4$ (M = Mo (**3**), W (**4**)), the singly reduced complex [W(bpy)(CO)$_4$][K(18-crown-6] (**5**) and the doubly
10 reduced complex [W(bpy-*t*Bu)(CO)$_3$][K(18-crown-6)]$_2$ (**6**) are reported. DFT calculations have been used to characterize the reduced species from the reduction of W(bpy-*t*Bu)(CO)$_4$ (**4**). These compounds represent rare examples of group 6 electrocatalysts for CO$_2$ reduction, and comparisons are made with the related group 7 complexes that have been studied extensively for CO$_2$ reduction.

Introduction

15 The electrocatalytic reduction of CO$_2$ to value-added products and fuels is an area that has seen significant progress over the last several decades.[1-5] In particular, the use of homogeneous electrocatalysts is an attractive approach because they can be studied with a variety of techniques and modified via synthesis to
20 affect reactivity. Previous work from our group focused on the study of complexes of the type M(bpy-R)(CO)$_3$X (M = Re, Mn; R = H, *t*Bu, etc.), based on the 2,2'-bipyridine system originally reported by Lehn[6]. Our more recent studies have shown that the 4,4'-di-*tert*-butyl-2,2'-bipyridine (bpy-*t*Bu) ligand is effective in
25 increasing the activity of rhenium-based CO$_2$ reduction catalysts compared to the complexes of their 2,2'-bipyridine counterparts.[7-9]

Many homogeneous electrocatalysts for CO$_2$ reduction are based on expensive and rare metals such as Ru and Re. The cost
30 of these metals makes it difficult to envision their use in large-scale deployment of systems for the synthesis of renewable chemicals and fuels from CO$_2$. Significant progress has been made towards developing electrocatalysts based on more abundant metals (for example: Mn,[10, 11] Ni,[12] Fe,[13, 14] and Cu[15]).
35 Notably, there are very few reports of electrocatalytic CO$_2$ reduction catalysts based on complexes of group 6 metals (Cr, Mo, W),[16, 17] even though this group contains the metals commonly found in the active sites of formate dehydrogenase (FDH) enzymes, which interconvert CO$_2$ and formate.[18] Aerobic
40 bacteria also utilize molybdenum in the active site of carbon monoxide dehydrogenase (CODH) enzymes that are capable of oxidizing CO to CO$_2$.[19]

Stoichiometric reactions of dianionic Cr, Mo and W pentacarbonyl complexes with CO$_2$ lead to the formation of
45 coordinated CO (Scheme 1),[20] and there are other examples of stoichiometric CO$_2$ reduction at homogeneous group 6 metal complexes.[21,22,23] The coupling of CO$_2$ with olefins,[24] as well as

hydrogenation of CO$_2$ to formic acid[25] or alkyl formates[26] have been observed at group 6 complexes. Given the precedent for
50 CO$_2$ reactivity with group 6 complexes, we were curious to see if 2,2'-bipyridine complexes of these group 6 metals could be used as *electrocatalysts* for the reduction of CO$_2$ to produce value-added products such as CO.
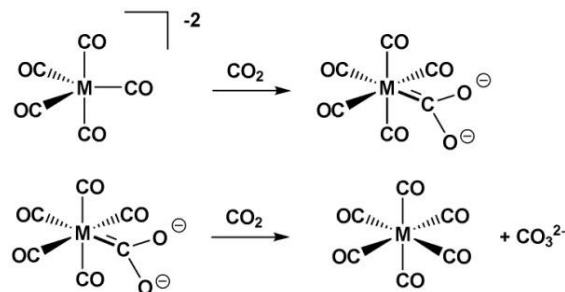
55
Scheme 1. Reactions of group 6 dianions with CO$_2$ (M = Cr, Mo, W).[20]

The spectroscopic, photochemical, and electrochemical properties of group 6 complexes of the type M(L)(CO)$_4$ (M = Cr,
60 Mo, W, L = diimine ligand) are well known.[27] It has been proposed that the reduction of these metal complexes by two electrons leads to the loss of a CO ligand and generation of a five-coordinate [M(L)(CO)$_3$]$^{2-}$ species,[27,28] although spectroscopic characterization of such species has not been
65 reported. We note the parallel between this postulated [M(L)(CO)$_3$]$^{2-}$ species and the dianionic [M(CO)$_5$]$^{2-}$ complexes reported by Cooper and co-workers to react with CO$_2$ to form M(CO)$_6$,[20] thus reducing CO$_2$ to CO. The group 6 dianionic [M(bpy-R)(CO)$_3$]$^{2-}$ complexes are also formally isoelectronic to
70 the five-coordinate [Re(bpy-*t*Bu)(CO)$_3$]$^-$ and [Mn(bpy-*t*Bu)(CO)$_3$]$^-$ anions, the critical intermediates that react with CO$_2$ in electrocatalytic reduction of CO$_2$ by Re(bpy-*t*Bu)(CO)$_3$X and

Mn(bpy-*t*Bu)(CO)$_3$X.[11]

Herein we report electrochemical studies of the group 6 complexes M(bpy-R)(CO)$_4$ (R = H, M = Mo (**1**), W (**2**); R = *t*Bu, M = Mo (**3**), W(**4**)). We find that these complexes are electrocatalysts for the reduction of CO$_2$. Particular focus is placed on complex **4**, as it is isoelectronic with previously published highly active rhenium and manganese systems. NMR spectroscopy, X-ray crystallography, and Density Functional Theory (DFT) studies are also used to examine the species relevant to catalytic CO$_2$ reduction. The comparisons between the group 6 and group 7 complexes contribute to a clearer understanding of the specific characteristics that lead to more active CO$_2$ reduction catalysts.

Results and Discussion

Synthesis and Characterization

The known complexes M(bpy-R)(CO)$_4$ (M = W, Mo; R = H, *t*Bu, **1**–**4**, Figure 1), were synthesized similar to literature procedures.[29] These complexes were isolated as bright orange-red (M = Mo) or dark red (M = W) air-stable solids. Although complex **4** has been mentioned in the literature,[30-32] it's ^{1}H and ^{13}C NMR spectra had not been previously reported, and this data is included in the ESI. The FT-IR spectra of these complexes display the standard four-signal pattern (2A$_1$, B$_1$, and B$_2$) in the υ(CO) region (1700–2100 cm^{-1}, Fig. S1 in the ESI) for tetracarbonyl complexes of this type with values that are in agreement with the literature (Table S1 in the ESI).[33, 34] The addition of the *t*Bu groups increases the solubility of **3** and **4** in organic solvents compared to **1** and **2**.
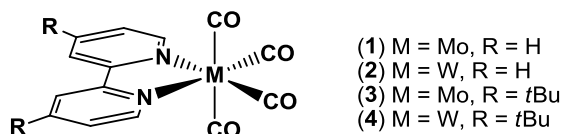

Figure 1. Tetracarbonyl complexes of molybdenum and tungsten examined in this work.

(**1**) M = Mo, R = H
(**2**) M = W, R = H
(**3**) M = Mo, R = *t*Bu
(**4**) M = W, R = *t*Bu

In order to compare with the reported X-ray structures of M(bpy)(CO)$_4$ (M = Mo (**1**)[35], W (**2**)[36, 37]), X-ray quality crystals were grown of the *tert*-butyl derivatives M(bpy-*t*Bu)(CO)$_4$ (M = Mo (**3**), W (**4**); see Figure 2) by vapor diffusion of pentane into concentrated toluene solutions of the complexes. The molecular geometries of **3** and **4** are similar to the corresponding complexes with the parent bipyridine ligand (**1** and **2**), with slightly shorter M–N bonds (Table S2), indicating slightly stronger donation from the *tert*-butyl ligand and slightly stronger back donation to the M–CO groups. This is also observed in the FT-IR data for complexes **1**–**4**, in which the υ(CO) frequencies are shifted to lower wavenumbers on the *t*Bu-substituted complexes compared to the parent complexes. The C–C bond lengths between the two pyridyl rings (C9–C10) for all of the complexes are consistent with a neutral bipyridine ligand.[38]

A search of the Cambridge Crystallographic Database did not yield any other tetracarbonyl tungsten or molybdenum complexes with 4,4'-disubstituted bipyridine ligands.[39] However, a comparison of the structures of **1**–**4** with previously reported

isoelectronic [Re(bpy-R)(CO)$_4$](OTf) complexes reveals interesting similarities and differences. The bending of the axial CO ligands away from the bipyridine ligands in complexes **1**–**4** (as seen in the M–C1–O1 and M–C4–O4 angles of *ca.* 171–172º) is a common feature of group 6 tetracarbonyl complexes, and has been explained in terms of back donation from a π* orbital on the bidentate diimine ligand.[40] This structural deviation of the metal carbonyls from linearity is also apparent in the structure of the d^6 [Re(bpy-R)(CO)$_4$](OTf) complexes (R = H, *t*Bu).[41, 42] Notably, complex **4** has significantly longer C–O bond lengths compared to [Re(bpy-*t*Bu)(CO)$_4$](OTf), which is evidence of stronger back donation from the tungsten metal center. This is also reflected in the FT-IR spectra of **4** and the corresponding rhenium complex. They have similar patterns for the υ(CO) stretches in their FTIR spectra, but the stretches for the tungsten complex **4** are 116–138 cm^{-1} lower in energy than the rhenium complex in acetonitrile.
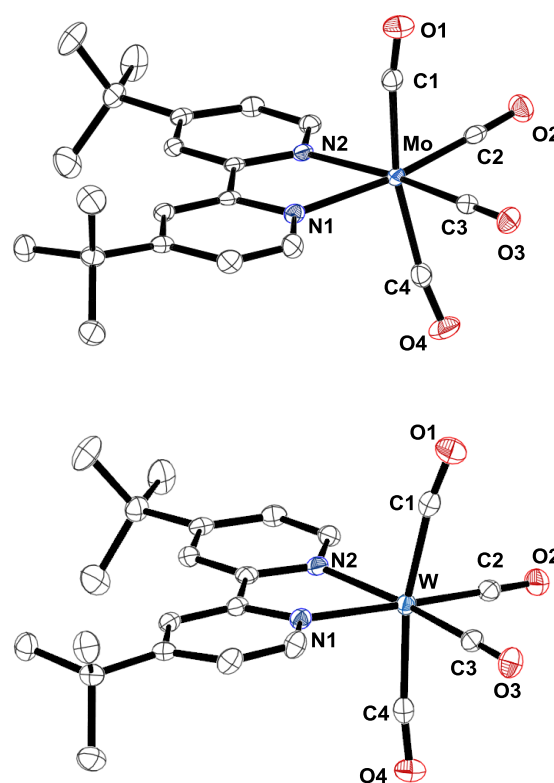
Figure 2. Molecular structures of **3** (top) and **4** (bottom), with ellipsoids shown at 50% probability and hydrogen atoms excluded for clarity. Selected bond lengths and angles are listed in Table S2 in the ESI.

Electrochemical Studies

The cyclic voltammograms of complexes **1**–**4** in acetonitrile are very similar, displaying one reversible reduction at ca. −1.6 V vs. SCE followed by an irreversible reduction at ca. −2.1 V vs. SCE (voltammogram for **1** shown in Figure 3, reduction potentials for **1**–**4** are listed in Table 1 and voltammograms of **2**-**4** Fig. S2). This data is similar to previously reported electrochemistry for **1** and **2** that was obtained in THF,[43, 44] acetonitrile (1st reduction only),[45] and dimethoxyethane.[46, 47] The first reduction of **3** has also been reported in multiple solvents.[48] The first reduction of these complexes is primarily localized on

the bipyridyl ligand, forming stable 19-electron [M(bpy-R)(CO)$_4$]$^{\cdot-}$ species that have been previously characterized for the parent bipyridine complexes **1** and **2** by FT-IR,[46] UV-Vis,[28] and EPR spectroscopies.[28, 49]

Table 1. Reduction potentials vs. SCE for complexes **1–4**. All complexes were studied under the same conditions as stated for **1**.

Complex	E$_{1/2}$ (V)	2nd (V)^a
1	−1.58	−2.14
2	−1.49	−2.08
3	−1.66	−2.20
4	−1.58	−2.15

^{a}Irreversible, reported as the location of the peak of the irreversible wave vs. SCE during the reductive sweep in the cyclic voltammogram at 100 mV/s.

When acetonitrile solutions containing complexes **1–4** are exposed to a CO$_2$ atmosphere, the first reduction in the cyclic voltammograms is similar to the reduction under inert atmosphere. However, at the second reduction potential, a current increase is observed (i$_{cat}$/i$_p$ = 2.3, 3.4, 3.1, and 3.9 for **1**, **2**, **3**, and **4**, respectively, Figure 3), which is attributed to catalytic reduction of CO$_2$. These current enhancements occur at potentials that are similar to the peak potential of CO$_2$ reduction by Re(bpy-*t*Bu)(CO)$_3$Cl (−2.1 V vs SCE).[7] The i$_{cat}$/i$_p$ and the corresponding turnover frequency (TOF, Table 2) show that the tungsten complexes are more active than the molybdenum complexes, and the *tert*-butyl groups enhance the activity for both metals. Complex **4** was selected for further study as it was the most active catalyst based on cyclic voltammetry (i$_{cat}$/i$_p$ of 3.9), but more importantly because it is isoelectronic with the well-studied fac-Re(bpy-tBu)(CO)$_3$X species so that the most appropriate comparison can be made.

Scan-rate dependence studies for complex **4** (Fig. S3 in the ESI) show that the second reduction remains irreversible even at high scan rates (ca. 10 V s^{-1}). The irreversibility of the second reduction indicates that a chemical reaction occurs following this reduction. This can be postulated as a loss of one CO ligand, although there is only brief mention of this in the literature, and full characterization for the dianions has not been previously reported.[28,27] The small oxidation wave observed at ca. −700 mV only appears after the second reduction is reached.
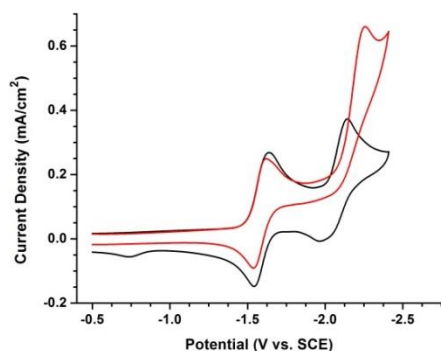
Figure 3. Representative cyclic voltammogram of **1** at a scan rate of 100

mV·s^{-1} under N$_2$ (black line) and CO$_2$ (red). Conditions: 1 mm diameter glassy carbon working electrode, platinum wire counter electrode, Ag/AgCl reference, decamethylferrocene (FeCp$_2$*) internal reference, 1 mM **1**, 0.1 M tetrabutylammonium hexafluorophosphate (TBAPF$_6$), room temperature. Complexes **2**, **3**, and **4** exhibit similar behavior (see ESI).

Controlled Potential Electrolysis

In order to study the catalytic reduction of CO$_2$, controlled potential electrolysis experiments were carried out with complex **4**. Care was taken to separate the counter electrode from the solution with a glass tube packed with a plug of glass wool during bulk electrolysis, because it has been shown that electrochemical oxidation of group 6 M(L)(CO)$_4$ complexes leads to the liberation of CO.[34] Bulk electrochemical reduction at −2.3 V under a CO$_2$ atmosphere led to formation of CO with a 109 ± 7% faradaic efficiency, as detected by gas chromatography (Fig. S4). Carbon monoxide was also observed by gas chromatography when the same experiment was performed under inert atmosphere, due to the loss of a carbonyl ligand that occurs after the second reduction. The current density under CO$_2$ initially decreased after the start of the bulk electrolysis but stabilized at 0.66 mA/cm^2, whereas under N$_2$ it stabilized at 0.44 mA/cm^2 (Fig. S5). This verifies the catalytic activity observed in the cyclic voltammograms, and also indicates that the catalyst is highly selective for CO formation. There was no evidence of carbonate, formate, or other CO$_2$-derived products by NMR or FT-IR measurements of complex **4**, and therefore the reaction is likely of the form CO$_2$ + 2e$^-$ + 2H$^+$ → CO + H$_2$O, similar to the group 7 catalysts. The catalytic activity was observed to be stable over the course of several hours (Fig. S6), indicating that the compound remains active over time. Hydrogen was observed only in small quantities (less than 3% faradaic efficiency).

Chemical Reduction and Characterization of the Reduced Species

Crystallographic characterization of the mono or di-reduced forms of M(bpy-R)(CO)$_4$ have not been reported, nor have the di-reduced species been characterized by spectroscopy. While the oxygen and proton sensitivity of these highly reduced forms makes isolation challenging, the anions and dianions of **2** and **4** were produced in yields of 40%−70% and characterized by FT-IR and NMR (ESI). After many attempts, crystal structures of the anion [W(bpy)(CO)$_4$]$^-$ (**5**) and dianion [W(bpy-*t*Bu)(CO)$_3$]$^{2-}$ (**6**) were obtained. Addition of 1 equivalent of KC$_8$ to a solution of **2** and 18-crown-6 in THF led to the formation of a dark orange solution of the new species **5**. Vapor diffusion of pentane into a solution of **5** in THF led to black-orange crystals suitable for X-ray diffraction. Consistent with analogous anionic complexes,[7, 8, 11] the anionic tungsten complex crystallizes with the potassium cation enclosed in the crown ether, seen in Figure 4. The potassium is both associated with an axial carbonyl (K–O bond length of 2.813(3) Å) and a THF solvent molecule. The bond length alteration in the 2,2'-bipyridine ring of **5** is suggestive of substantial electron density on the ligand, supporting the assignment of the first electrochemical reduction as being ligand based.[50]
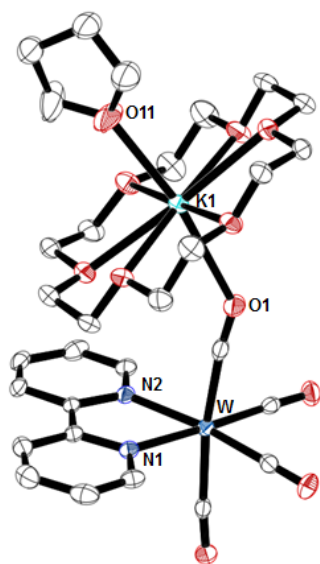
Figure 4. Molecular structure of [W(bpy)(CO)$_4$][K(18-crown-6)•THF] (**5**). Ellipsoids are shown at 50% probability. Hydrogen atoms are omitted for clarity.

Dianionic species **6** was formed by the addition of 2.2 equivalents of KC$_8$ to a THF solution of **4** in the presence of 18-crown-6. The ^{1}H NMR spectrum of the black-purple solution of complex **6** in THF-d_8 (Fig. S9) showed signals for a diamagnetic compound, with bipyridine ligands that were significantly shifted upfield from the starting material (4.80, 6.60, and 8.47 ppm for **6** vs. 7.58, 8.40, and 9.10 ppm for **4**). This upfield shift in the C–H protons on the bipyridine ligand has also been observed in the [Al(bpy-H)$_2$]$^-$ anion, which has been assigned as possessing two (bpy-H)$^{2-}$ ligands.[51]
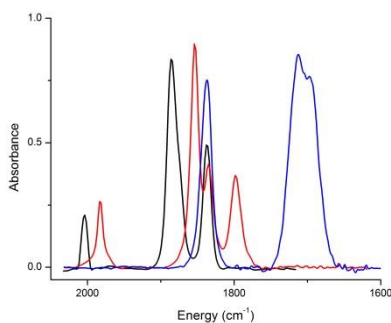
Figure 5. FTIR spectra of the chemically reduced species of W(bpy-tBu)(CO)$_4$ (**4**) in THF under N$_2$. The neutral species **4** (black) has υ(CO) stretches of 2004 cm^{-1}, 1886 cm^{-1}, and 1837 cm^{-1}. The chemically reduced anion (red) υ(CO) stretches are 1982 cm^{-1}, 1854 cm^{-1}, 1835 cm^{-1}, and 1798 cm^{-1}; the doubly reduced species **6** (blue) υ(CO) stretches are 1837 cm^{-1} and 1713 cm^{-1}.

A diffracting crystal of **6** was obtained after multiple crystallization attempts. Although several issues exist with the structure, it was found to be the [W(bpy-tBu)(CO)$_3$][K(18-crown-6)]$_2$ species. The dianion crystallizes between two layers of the 18-crown-6 ligands, which display significant disorder (Fig. S7 in the ESI). The C9–C10 distance in **6** is significantly shorter than the corresponding bond in **4** (1.483 Å). The C–O distances in the carbonyl ligands of **6** are also significantly longer than those in **4**.

The lengthening of the metal-carbonyl bonds in **5** and **6** due to the increased back bonding from the metal is consistent with the FT-IR spectra of these complexes. The carbonyl stretching frequencies of complex **4** shift to a lower frequency by roughly 30 cm^{-1} upon the first chemical reduction, and the subsequent reduction leads to the dianion **6**, which exhibits a band at 1837 cm^{-1} and a broad band at 1713 cm^{-1} as shown in Figure 5 (the IR spectra of **5** and of the dianion [W(bpy)(CO)$_3$]$^{2-}$ are shown in Fig. S8 in the ESI). These υ(CO) bands are observed at much lower frequencies than [Re(bpy-tBu)(CO)$_3$]$^-$ (1940 cm^{-1} and 1835 cm^{-1}) and Mn(bpy-tBu)(CO)$_3$]$^-$ (1911 cm^{-1} and 1813 cm^{-1}) anions that are isoelectronic with **6**. This indicates that the anion **6** has much stronger back donation to the antibonding π* orbitals of the CO ligands than the corresponding Re or Mn monoanions with the same ligand sets.

DFT Calculations of Catalytically Relevant Complexes

In order to obtain a deeper insight into the species formed upon electrochemical reduction of **4**, the DFT-optimized structures of the reduced species obtained from **4** were calculated. Geometry optimized structures were obtained by using the X-ray coordinates of **4** and **6** as the initial inputs to obtain the structures of the neutral form (**A**) and the five-coordinate dianion (**D**). The geometry of the mono-reduced species [W(bpy-tBu(CO)$_4$]$^{-1}$ (**B**) and the doubly-reduced species structure [W(bpy-tBu)(CO)$_4$]$^{-2}$ (**C**) were then optimized from **A** (Scheme 2). Frequency calculations were used to establish that the optimized structures were not intermediates. The crystal structure for **6** and the DFT-optimized structure of **D** are intermediate between a square pyramid and a trigonal bipyramid (τ_5 = 0.44 and 0.46, respectively)[52] (Figure 5). Pertinent bond distances for the calculated structures and coordinates for the optimized structures are included in the ESI. The calculated υ(CO) stretching frequencies for species **D** (1822, 1734, and 1724 cm^{-1}) agree well with the υ(CO) band energies observed in IR for the reduced species **6** in THF (1837 cm^{-1} and a broad band at 1713 cm^{-1}). A comparison of the calculated and experimental υ(CO) stretching frequencies for species **A–D** is included in the ESI (Table S5). The central C–C bonds in the bipyridine ligands in the dianions **C** and **D** are significantly shortened compared to **A** and **B**, with C–C bond lengths of 1.390 and 1.398 Å for the central C–C bond in the bipyridine ligand in the octahedral (**C**) and five-coordinate (**D**) complexes. The bond lengths for **C** and **D** are shorter than the bond lengths in the neutral complex (1.463 and 1.481 Å for geometry optimization (**A**) and X-ray structure of **4**), and the monoanion (**B**) (1.423 Å). These results are consistent with our understanding of the system from the electrochemical and structural studies, indicating that the bipyridine accepts a significant amount of the electron density from both 1e$^-$ reductions observed in the electrochemistry of **1–4**.
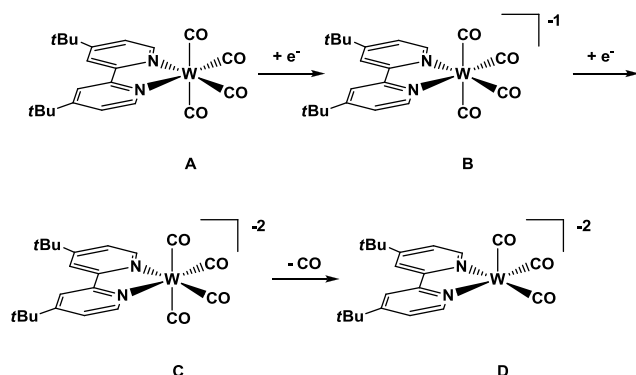
Scheme 2. Complexes based on complex **4** that were studied using DFT calculations.

Examination of the calculated highest occupied molecular
orbitals (HOMOs) and lowest unoccupied molecular orbitals
(LUMOs) of complexes **A**–**D** provides further insights about
these complexes. The calculated HOMO of the dianion **D** is
delocalized over the bipyridine and somewhat over the tungsten
center (Figure 6). In comparison, the LUMO, singly occupied
molecular orbital (SOMO) and HOMO of **A**, **B**, and **C** are
primarily localized on the bipyridine with some electron density
on the CO ligands (see ESI). The calculated HOMO for species **D**
is qualitatively similar to the calculated HOMO for the [Re(bpy-
tBu)(CO)$_3$]$^{-1}$ anion, which is the reactive species in catalysis with
Re(bpy-tBu)(CO)$_3$X catalysts.[8] Calculations on a related species,
[Mn(bpy-H)(CO)$_3$]$^{-1}$ also showed that the HOMO of this species
is delocalized over the bipyridine ligand as well as the metal
center.[53]
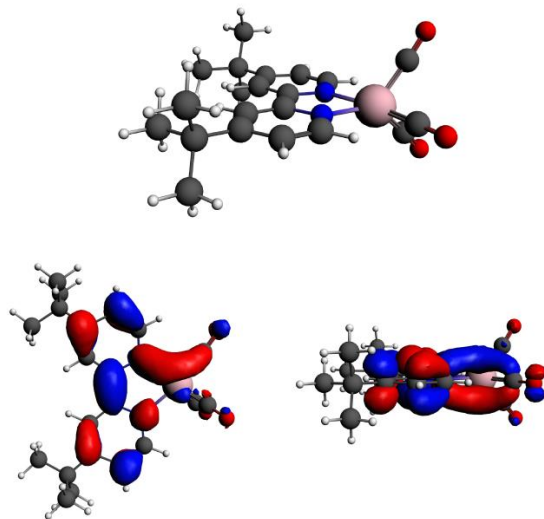
Figure 6. Ball and stick representation of the geometry optimized
structure (top) and the DFT-calculated HOMO (bottom left: top view;
right: side view) of the five-coordinate dianionic species **D**.

Comparison with Group 7 Catalysts

A comparison of the catalytic activities of **1**–**4** with analogous
group 7 complexes is shown in Table 2. The group 6 species are
similar in activity to [Re(bpy-tBu)(CO)$_3$(CH$_3$CN)](OTf) and

more active than the corresponding Mn species under the same
conditions (Mn complexes do not exhibit catalysis without added
protons). Upon the addition of a proton source, the group 7
catalysts greatly outperform the W and Mo species. The effect of
adding a Brönsted acid could not be quantified for the group 6
species due to the negative potentials of the second reductions
being too close to the direct reduction of the acids at the
electrodes in the cyclic voltammetry experiments.

While the Mo and W complexes reported herein are not
exceptional electrocatalysts for CO$_2$ reduction, their study is very
valuable because it provides a framework in which to understand
similar electrocatalysts, such as the group 7 species. Through
comparisons of the structurally similar and isoelectronic group 6
M(bpy-R)(CO)$_4$ species and the group 7 M(bpy-R)(CO)$_3$X
species, we can understand what characteristics lead to efficient
and active catalysts.

The first electrochemical reduction of both the group 6 (**1**-**4**)
and group 7 M(bpy-R)(CO)$_3$X (M = Re, Mn) electrocatalysts
proceeds through reduction of the bipyridine ligand. In the
rhenium system, ligand loss (dissociation of the chloride or other
X ligand) subsequently occurs from [Re(bpy-R)(CO)$_3$X]$^-$ leading
to a species that can be assigned as a Re(0) center and a neutral
bipyridine ligand. Ultimately, a Re(0)–Re(0) dimer is formed,
and characterization of the dimer gives clear indication that the
reduction has occurred at the metal center.[54] For manganese,
reduction of a Mn(bpy-R)(CO)$_3$X species leads to extremely
rapid dimerization such that monomeric [Mn(bpy-R)(CO)$_3$X]$^-$
species have not been observed spectroscopically. In stark
comparison, the group 6 complexes do not lose a ligand or
dimerize upon reduction, but rather the axial carbonyl becomes
somewhat more susceptible to substitution.[43] However, the
electron density remains primarily over the bipyridine ligand, and
the carbonyl ligand remains strongly coordinated enough that we
were able to crystallize the [W(bpy)(CO)$_4$]$^-$ anion (complex **5**),
wherein the bipyridine ligand is clearly reduced. Notably,
reduction of a [Re(bpy-R)(CO)$_4$]$^+$ cation does not lead to an
observable Re(bpy-R)(CO)$_4$ species,[42] indicating that the group 6
complexes bind CO more strongly than the group 7 complexes.

A second reduction in both the group 6 and the group 7
systems leads to a diamagnetic complex with five-coordinate
geometry and a similar HOMO delocalized over the metal and the
bipyridine. For the rhenium complexes, XANES data suggests
that these species are best described as M^0(bpy^{-1}). The second
reduction in the Re(bpy-R)(CO)$_3$Cl systems is 300–400 mV more
negative than the first, however the second reduction potentials of
1–**4** are 540–590 mV more negative than their first reduction.
This is similar to the separation observed between the 2,2'-
bipyridine monoanion and dianion.[55] Thus it seems reasonable
that they are described as M^0(bpy^{-2}) species, rather than M^{-1}(bpy^{-1}) or M^{-2}(bpy^0) complexes. Further studies are needed to
unambiguously assign these ground states.

Table 2. Comparison of the catalytic activity of complexes **1-4** to relevant group 7 complexes.[11]

Complex	i_{cat}/i_p	TOF $(s^{-1})^a$
$Mo(bpy)(CO)_4$ **(1)**	2.3	1.0
$W(bpy)(CO)_4$ **(2)**	3.4	2.2
$Mo(bpy\text{-}tBu)(CO)_4$ **(3)**	3.1	1.9
$W(bpy\text{-}tBu)(CO)_4$ **(4)**	3.9	2.9
$[Re(bpy\text{-}tBu)(CO)_3(CH_3CN)](OTf)^b$	3.3	2.1
$Mn(bpy\text{-}tBu)(CO)_3Br^b$	1.0	0.0
$[Re(bpy\text{-}tBu)(CO)_3(CH_3CN)](OTf)^c$	54	570
$Mn(bpy\text{-}tBu)(CO)_3Br^d$	42	340

^{a}TOF for **1-4** obtained using method described by Smieja et al.[11] ^{b}Activity under similar conditions to those used for **1-4**. ^{c}1.4 M 2,2,2-trifluoroethanol (TFE) added. ^{d}1.6 M TFE added.

These comparisons lead to two important conclusions about electrocatalysts for CO_2 reduction. The first is that having catalytically relevant electrons stored in both the bipyridine ligand and the metal center leads to a lower overpotential compared to having two electrons stored on the bipyridine ligand. The second conclusion about these electrocatalysts is that having a complex that strongly back-donates to CO is undesirable because it will hinder release of the product and slow overall catalysis, *i.e.* CO poisoning of the catalyst.

Conclusions

Electrochemical experiments on groups 6 complexes **1–4** $M(bpy\text{-}R)(CO)_4$ (R = H, M = Mo (**1**), W (**2**); R = *t*Bu, M = Mo (**3**), W (**4**)) have shown that these complexes are competent catalysts for CO_2 reduction through a two-electron reduction process to generate a diamagnetic dianionic complex. The reduced species have been studied using X-ray crystallography, IR spectroscopy and DFT calculations. These catalysts display stronger back donation to CO than group 7 catalysts, which may explain why they operate at slower rates. Future studies will include studying the stoichiometric reactions of the reduced species with CO_2 and H^+ sources, as well as attempting to elucidate the full catalytic cycle. The catalytic cycle of CO_2 reduction by $Re(bpy)(CO)_3Cl$ has recently been elucidated by computational methods, and similar study of group 6 catalysts would be very informative.[56] Complexes **1–4** are rare examples of group 6 electrocatalysts for CO_2 reduction and future work will focus on developing more efficient and selective catalysts based on these relatively abundant metals.

Acknowledgements

Notes and references

Department of Chemistry and Biochemistry, University of California, San Diego, 9500 Gilman Drive MC 0358, La Jolla, California 92093, USA. E-mail: ckubiak@ucsd.edu; Fax: 01 858 534 5383; Tel: 01 858 822 2665

1. E. E. Benson, C. P. Kubiak, A. J. Sathrum and J. M. Smieja, *Chem. Soc. Rev.*, 2009, **38**, 89-99.
2. J.-M. Savéant, *Chemical reviews*, 2008, **108**, 2348-2378.
3. C. D. Windle and R. N. Perutz, *Coordination Chemistry Reviews*, 2012, **256**, 2562-2570.
4. C. Costentin, M. Robert and J.-M. Saveant, *Chemical Society reviews*, 2013, **42**, 2423-2436.
5. A. M. Appel, J. E. Bercaw, A. B. Bocarsly, H. Dobbek, D. L. DuBois, M. Dupuis, J. G. Ferry, E. Fujita, R. Hille, P. J. A. Kenis, C. A. Kerfeld, R. H. Morris, C. H. F. Peden, A. R. Portis, S. W. Ragsdale, T. B. Rauchfuss, J. N. H. Reek, L. C. Seefeldt, R. K. Thauer and G. L. Waldrop, *Chemical reviews*, 2013, **113**, 6621-6658.
6. J. Hawecker, J. M. Lehn and R. Ziessel, *J. Chem. Soc., Chem. Commun.*, 1984, 328-330.
7. J. M. Smieja and C. P. Kubiak, *Inorg. Chem.*, 2010, **49**, 9283-9289.
8. J. M. Smieja, E. E. Benson, B. Kumar, K. A. Grice, C. S. Seu, A. J. Miller, J. M. Mayer and C. P. Kubiak, *Proceedings of the National Academy of Sciences of the United States of America*, 2012, **109**, 15646-15650.
9. K. A. Grice and C. P. Kubiak, in *Advances in Inorganic Chemistry*, eds. A. Michele and E. Rudi van, Academic Press, 2014, vol. Volume 66, pp. 163-188.
10. M. Bourrez, F. Molton, S. Chardon-Noblat and A. Deronzier, *Angewandte Chemie, International Edition*, 2011, **50**, 9903-9906.
11. J. M. Smieja, M. D. Sampson, K. A. Grice, E. E. Benson, J. D. Froehlich and C. P. Kubiak, *Inorganic Chemistry*, 2013, **52**, 2484-2491.
12. J. D. Froehlich and C. P. Kubiak, *Inorg. Chem.*, 2012, **51**, 3932-3934.
13. I. Bhugun, D. Lexa and J.-M. Savéant, *The Journal of Physical Chemistry*, 1996, **100**, 19981-19985.
14. C. Costentin, S. Drouet, M. Robert and J.-M. Savéant, *Science*, 2012, **338**, 90-94.
15. A. M. Lilio, K. A. Grice and C. P. Kubiak, *European Journal of Inorganic Chemistry*, 2013, **2013**, 4016-4023.
16. J. A. Ramos Sende, C. R. Arana, L. Hernandez, K. T. Potts, M. Keshevarz-K and H. D. Abruna, *Inorganic Chemistry*, 1995, **34**, 3339-3348.
17. C. J. Pickett and D. Pletcher, *J Chem Soc Dalton*, 1976, 749-752.
18. T. Reda, C. M. Plugge, N. J. Abram and J. Hirst, *Proceedings of the National Academy of Sciences*, 2008, **105**, 10654-10658.
19. H. Dobbek, L. Gremer, R. Kiefersauer, R. Huber and O. Meyer, *Proceedings of the National Academy of Sciences*, 2002, **99**, 15971-15976.
20. G. R. Lee, J. M. Maher and N. J. Cooper, *Journal of the American Chemical Society*, 1987, **109**, 2956-2962.
21. U. Jayarathne, P. Chandrasekaran, H. Jacobsen, J. T. Mague and J. P. Donahue, *Dalton Transactions*, 2010, **39**, 9662-9671.
22. L. Contreras, M. Paneque, M. Sellin, E. Carmona, P. J. Perez, E. Gutierrez-Puebla, A. Monge and C. Ruiz, *New Journal of Chemistry*, 2005, **29**, 109-115.

Chemical Science Accepted Manuscript

23. B. L. Yonke, J. P. Reeds, P. Y. Zavalij and L. R. Sita, *Angewandte Chemie International Edition*, 2011, **50**, 12342-12346.

24. W. H. Bernskoetter and B. T. Tyler, *Organometallics*, 2011, **30**, 520-527.

25. C.-C. Tai, T. Chang, B. Roller and P. G. Jessop, *Inorganic Chemistry*, 2003, **42**, 7340-7341.

26. D. J. Darensbourg and C. Ovalles, *Journal of the American Chemical Society*, 1984, **106**, 3750-3754.

27. A. n. Vlček Jr, *Coordination Chemistry Reviews*, 2002, **230**, 225-242.

28. Y. Kaizu and H. Kobayashi, *Bulletin of the Chemical Society of Japan*, 1972, **45**, 470-477.

29. T. S. A. Hor and S.-M. Chee, *Journal of Organometallic Chemistry*, 1987, **331**, 23-28.

30. E. Tolun, C. J. Proctor, J. F. J. Todd, J. M. A. Walshe and J. A. Connor, *Organic Mass Spectrometry*, 1984, **19**, 294-294.

31. M. J. Schadt and A. J. Lees, *Inorganic Chemistry*, 1986, **25**, 672-677.

32. S. Cao, K. Bal Reddy, E. M. Eyring and R. van Eldik, *Organometallics*, 1994, **13**, 91-93.

33. J. A. Connor and C. Overton, *Journal of Organometallic Chemistry*, 1983, **249**, 165-174.

34. R. Johnson, H. Madhani and J. P. Bullock, *Inorganica Chimica Acta*, 2007, **360**, 3414-3423.

35. S. S. Braga, A. C. Coelho, I. S. Goncalves and F. A. Almeida Paz, *Acta Crystallographica Section E*, 2007, **63**, m780-m782.

36. Q. Ye, Q. Wu, H. Zhao, Y.-M. Song, X. Xue, R.-G. Xiong, S.-M. Pang and G.-H. Lee, *Journal of Organometallic Chemistry*, 2005, **690**, 286-290.

37. J. Chapman, G. Kolawole, N. Long, A. J. P. White, D. J. Williams and P. O'Brien, *S. Afr. J. Sci.*, 2005, **101**, 454-456.

38. C. C. Scarborough and K. Wieghardt, *Inorganic Chemistry*, 2011, **50**, 9773-9793.

39. F. Allen, *Acta Crystallographica Section B*, 2002, **58**, 380-388.

40. C. Makedonas and C. A. Mitsopoulou, *European Journal of Inorganic Chemistry*, 2007, **2007**, 110-119.

41. T. Scheiring, W. Kaim and J. Fiedler, *Journal of Organometallic Chemistry*, 2000, **598**, 136-141.

42. K. A. Grice, N. X. Gu, M. D. Sampson and C. P. Kubiak, *Dalton Transactions*, 2013, **42**, 8498-8503.

43. D. Miholová and A. A. Vlček, *Journal of Organometallic Chemistry*, 1985, **279**, 317-326.

44. D. Miholová, B. Gaš, S. Záliš, J. Klíma and A. A. Vlček, *Journal of Organometallic Chemistry*, 1987, **330**, 75-84.

45. R. J. Crutchley and A. B. P. Lever, *Inorganic Chemistry*, 1982, **21**, 2276-2282.

46. R. E. Dessy and L. Wieczorek, *Journal of the American Chemical Society*, 1969, **91**, 4963-4974.

47. R. E. Dessy, F. E. Stary, R. B. King and M. Waldrop, *Journal of the American Chemical Society*, 1966, **88**, 471-476.

48. J. A. Connor, C. Overton and N. El Murr, *Journal of Organometallic Chemistry*, 1984, **277**, 277-284.

49. J. A. Vlcek, F. Baumann, W. Kaim, F.-W. Grevels and F. Hartl, *Journal of the Chemical Society, Dalton Transactions*, 1998, 215-220.

50. E. Gore-Randall, M. Irwin, M. S. Denning and J. M. Goicoechea, *Inorg. Chem.*, 2009, **48**, 8304.

51. G. B. Nikiforov, H. W. Roesky, M. Noltemeyer and H. G. Schmidt, *Polyhedron*, 2004, **23**, 561.

52. A. W. Addison, T. N. Rao, J. Reedijk, J. van Rijn and G. C. Verschoor, *Journal of the Chemical Society, Dalton Transactions*, 1984, 1349-1356.

53. F. Hartl, P. Rosa, L. Ricard, P. Le Floch and S. Záliš, *Coordination Chemistry Reviews*, 2007, **251**, 557-576.

54. E. E. Benson and C. P. Kubiak, *Chemical communications*, 2012, **48**, 7374-7376.

55. M. Krejčik and A. A. Vlček, *Journal of Electroanalytical Chemistry and Interfacial Electrochemistry*, 1991, **313**, 243-257.

56. J. A. Keith, K. A. Grice, C. P. Kubiak and E. A. Carter, *Journal of the American Chemical Society*, 2013, **135**, 15823-15829.